

Effect of Hydride on the Mechanical Property of PT-7M Titanium Alloy

Tae-Kyu Kim, Jong-Hyuk Baek, Yong-Hwan Jeong, Doo-Jeong Lee, Moon-Hee Chang

Korea Atomic Energy Research Institute
P.O.Box 105, Yusung, Taejon 305-600, Korea

ABSTRACT

The effect of hydride on the mechanical property of PT-7M titanium alloy has been evaluated. Room temperature tensile tests were performed at a constant crosshead speed of 0.127mm/sec. Tensile test results indicated that there was little effect of hydrogen content on the yield strength and ultimate tensile strength of titanium alloy. However, the hydride precipitation of the δ phase (TiH_2) in this alloy offered a source for crack initiation and propagation in the presence of stress, leading to the cleavage failure mode. It resulted in a serious loss of the ductility as the hydrogen content increased

1. INTRODUCTION

It is well known that titanium alloys have the high specific strength including that at elevated temperature, unique corrosion resistance to many mineral acids and chlorides, low disposition to vacancy swelling, low disposition to be activated in neutron flux, and suitable durability characteristics [1-3]. It resulted in rather a wide application of these alloys in aerospace, chemical, petrochemical, and shipbuilding industries [4-8].

A significant attention has been directed towards the hydrogen embrittlement of titanium alloys, because titanium is usually used in many applications where hydrogen is present in water solution. When titanium alloys are exposed to water, some of the hydrogen resulting from the reaction of titanium alloys with water to form TiO_2 is absorbed by the metal [9]. Hydrogen absorbed may enter the lattice of the metal, and usually forms a hydride. The presence of quite small amounts of hydrogen in titanium alloys can result in serious loss of mechanical properties such as ductility, impact strength, notch tensile strength, and creep resistance [10-15].

Unfortunately, there is little identification about the effect of hydride content on the mechanical property of PT-7M titanium alloy. It is expected that the mechanical property of the PT-7M

titanium alloy tube, when it contains the hydrogen as a form of hydride precipitation, is dependent on the hydrogen content. This study has been performed to evaluate the effect of hydrogen content on the mechanical property of PT-7M titanium alloy. The variation of hydrogen content for the alloy has been principally achieved using a hydrogen charging system.

PT-7M: CAS Registry number 66082-54-0 (American Chemical Society)

2. EXPERIMENTAL PROCEDURES

PT-7M titanium alloy tubes (150 mm L. \times 6 mm I.D. \times 10 mm O.D. in size) were prepared. The chemical composition of the alloy examined in the present study is given in Table 1. Its microstructure was examined by a Transmission Electron Microscope (TEM). The alloy was exposed to a solution with a chemical composition (45H₂O:45HNO₃:10HF in wt.%) for 10 seconds to remove the oxide layer on its outer surface.

Fig. 1 shows a schematic diagram of the hydrogen charging equipment used in this study. The alloy tube was placed in the uniform temperature zone of the furnace, and then was induction heated at a rate of 10 °C/min in a high vacuum degree of 4×10^{-6} torr. When the temperature of the alloy tube reached to 500 °C, the hydrogen gas was charged until the pressure of hydrogen met to be 500 torr. Then, the alloy was held for 5, 10, 13, 20, 30 and 60 min, respectively. The hydrogen charged alloys were furnace cooled at an extremely slow cooling rate of 1 °C/min in a vacuum degree of 4×10^{-6} torr. to avoid a supersaturation of hydrogen in the matrix. For the homonization of the hydrogen in the hydrided tubes, it was also heat treated at 400 °C for 2 hours. The tensile tests of the hydrogen charged alloys at room temperature were carried out at a constant crosshead speed of 0.127 mm/sec. Tensile test of the alloy with the same thermal history were also performed to evaluate only the effect of heat treatment on the mechanical property of this alloy. The effect of hydrogen content on the hardness of the alloys was also evaluated.

The hydrogen contents of hydrogen charged alloys were analyzed. Microstructures of hydrogen charged alloys were observed using a scanning electron microscopy (SEM), and the crystal structure of hydride precipitation was examined using a X-ray diffraction (XRD) pattern. The fractured surfaces and longitudinal sections of the samples tested were also examined using a SEM.

3. RESULTS AND DISCUSSION

3.1 Microstructure

Fig. 1 shows a bright field TEM image in longitudinal section of PT-7M titanium alloy tube. It

is observed that this alloy has a fully recrystallization structure of α titanium alloy with an average grain size of about 20 μm . No β phase is observed. This reflects that the final annealing after the final pilgering stage in the manufacturing procedures of this alloy would be below a α - β transition temperature in Ti-Al-Zr ternary alloy system.

3.2 Hydrogen charging

The hydrogen contents of as-received and hydrogen charged PT-7M titanium alloys are given in Table 2. The hydrogen contents of titanium alloys appeared to be dependent on the hydrogen charging time in an atmosphere with a hydrogen pressure of 500 torr. The hydrogen contents increased by hydrogen charging i.e from 47 ppm in the as-received alloy to 1174 ppm after a charging time of 30 min, and further up to 2291 ppm after a charging time of 60 min.

Fig. 3 shows the variation of hydrogen pressure with charging time in a hydrogen charging system. It is observed that the pressure of hydrogen is exponentially reduced with the charging time. This means that the reduction of hydrogen pressure induced the increase of hydrogen content as a result of hydrogen diffusion into PT-7M titanium alloy. It is interesting to notice that the rate of hydrogen uptake into the alloy is almost constant, because the hydrogen content revealed to be directly correlated with the reduction of hydrogen pressure.

Fig. 4 shows surface appearance of as-received and hydrogen charged PT-7M titanium alloy tubes with hydrogen contents of 1174 and 2291 ppm. The hydrogen charged alloy tubes revealed to be a yellow color in their surfaces, as compared with the as-received one. In addition, they showed the more dense yellow color as hydrogen content increased.

3.3 Hydride

Fig. 5 shows the microstructures of hydrogen charged PT-7M titanium alloys. Because hydrogen solubility increases significantly with temperature, the alloys cooled from a high temperature can easily contain large amount of hydrogen which either remain in a supersaturated solution or precipitate as hydrides. It is observed that the amount of the hydride in the hydrogen charged alloys increased with increasing hydrogen content. The hydride in the alloy with a hydrogen content of 102 ppm showed finely dispersed particles mostly in the matrix as well as some lath-type morphology at the grain boundaries. In the alloy with a hydrogen content of 1174 ppm, the lath-type hydride considerably developed mostly at the grain boundaries, but occasionally in the matrix, as well as a spherical morphology mostly in the matrix. With respect to the size of hydride, a significant difference was observed; approximately less than 60 μm in the alloy with a hydrogen content of 102 ppm and approximately 200 μm in the alloy with a hydrogen content of 1174 ppm.

Fig. 6 shows an X-ray diffraction pattern for hydrogen charged PT-7M titanium alloys with hydrogen content of 1174 ppm. The phase identification of the hydrogen charged titanium alloy showed that this alloy composed of two phases; the α matrix with a crystal structure of

hexagonal close-packed (hcp, $a = 0.2950$ nm, $c = 0.4686$ nm) and the δ phase hydride (TiH_2) with a crystal structure of face-centered cubic (fcc, $a = 0.440$ nm). The δ hydride is a stable phase at ambient temperature, having the smallest atomic percent of 51.2% at eutectoid reaction temperature, 300 °C, in Ti-H binary system [16]. In Ti-H binary system, the solubility of hydrogen in pure Ti shows about 20-30 ppm range at room temperature. Thus, it is considered that the solubility of PT-7M titanium alloy (Ti-Al-Zr ternary system) would be less than 100 ppm, because the alloy with a hydrogen content of 102 ppm showed a large size of hydride.

3.4 Effect of hydrogen content on the tensile property

Fig. 7 shows the effect of hydrogen content on the mechanical property of PT-7M titanium alloys. PT-7M titanium alloys showed average yield strength values of 350 MPa with little variation as hydrogen content increased. For the ultimate tensile strength, the similar tendency (average values of 570 MPa) is observed, even if hydrogen is charged or not. These results indicate that there is little effect of hydrogen content on the strengths of titanium alloys. It is considered that the hydride acts as an obstacle for moving of dislocation during deformation, because the strength is almost decided by the dislocation movement at room temperature. However, there was a significant reduction of ductility of PT-7M titanium alloy as hydrogen content increased. The elongation values are gradually decreased with increasing hydrogen content. The elongation value of the alloy with a hydrogen content of 1194 ppm revealed to be 0.4%, whereas the as-received alloy showed an elongation value of 25% at room temperature. This means that a formation of the hydride precipitates of δ phase induced a considerable reduction of ductility in titanium alloy. These results indicate that the presence of hydride is of fundamental importance in ductility, and that the extent of hydride has a considerable influence on the ductility of titanium alloys. It is possible to explain that these low ductility values of hydrogen charged alloys in the present study are closely associated with the hydride precipitation of δ phase.

Fig. 8 shows SEM micrographs of the fracture surfaces of the as-received and hydrogen charged PT-7M titanium alloys. An examination of tensile tested titanium alloys using a SEM revealed the morphology of fracture surfaces was intimately associated with the hydride content identified as the δ phase hydride, and the fracture mode was changed from ductile to cleavage as hydrogen content increased. In Fig. 8(a), illustrating the ductile rupture, large voids are apparent on the fracture surface. The large voids are originally intergranular cracks formed by grain boundary sliding at an early stage of deformation. As deformation proceeds, the original grain boundary crack is distorted into an elongated void, until final failure occurs by necking between the voids. Fracture does not appear to be associated with a hydride, since grain boundary sliding appears to occur during deformation. However, it is observed in Fig. 8 (a)-(d) that an average depth of voids decreases with increasing the hydrogen content. In Fig. 8(e),

representing the brittle fracture, the fracture appeared to occur mainly in the matrix. It is also possible to observe that hydrides within the grain remain in the cavities, characteristic of precipitation-controlled failure.

Fig. 9 shows SEM images in the vicinity of the longitudinal sections of tensile tested PT-7M titanium alloys with hydrogen contents of 69, 102 and 1174 ppm. It is observed that the hydrides offer a source for crack initiation and propagation in the presence of stress at room temperature. The hydride particles would be under enhanced strain localization during deformation. In addition, there would be an effect of matrix/hydride interfacial tension depending on the matrix/hydride lattice mismatch, because a fcc δ hydride would not be coherent with the matrix which has a hcp structure. The hydrides are incoherent with α -titanium and have about a 23% larger specific volume. The α/δ interface would hence be weaker than the surrounding matrix during hot deformation, tending to fracture prior to the onset of grain boundary sliding (Fig. 9). Thus, it is considered that the low-ductility cleavage and intergranular fracture mode observed in the hydrogen charged PT-7M alloy are mainly attributed to the hydrides within the grains and in the grain boundaries (Figs. 7 and 8). There was no evidence of dynamic recrystallization during deformation in all alloys tested in the present study. It is thus possible to predict that ductility would always be improved when the hydrides are absent, thus preventing fracture initiation and facilitating grain boundary sliding. As a consequence, the hydride precipitates would have been sufficient to delay the onset of grain boundary sliding until a fracture had occurred, giving rise to low ductility. With respect to the directionality of hydride, it has very important characteristics to decide the mechanical property of titanium alloy tube. The hydride in the radius direction of the alloy tube shows a significant effect on the tensile property, and it is usually estimated as a Fn number. The tensile properties of hydrogen charged alloys in the present study have been almost decided by their hydrogen contents, because they had a similar Fn number. The detrimental effect of hydride on the ductility of titanium alloy coincides well with other results that the presence of hydride phases influences the mechanical properties of titanium alloys [10-15].

It is necessary to isolate the effect of heat treatment on the tensile property of as-received alloy, because the alloys are heat treated at 500°C for the hydrogen charging and at 400°C for homonization of hydrogen. The effect of heat treatment on grain size of PT-7M alloy revealed that the grain size increased by heat treatment i.e from about 20 μ m in the as-received alloy to about 22 μ m in the heat treated sample. Fig. 10 shows the effect of heat treatment on the mechanical property of PT-7M titanium alloy. The results demonstrate that the enlargement in grain size induces little effect of tensile test results. These results reflect that heat treatment shows little or no effect on the mechanical property of PT-7M titanium alloy. Based on this result, the tensile test results shown in Fig. 7 imply that all of effects on the mechanical properties of PT-7M titanium alloys is attributed to the hydrogen content.

3.5 Effect of hydrogen content on the Hardness

Fig. 11 shows the effect of hydrogen content on Vickers hardness of PT-7M titanium alloys. It can be seen that the hardness of PT-7M titanium alloys is directly dependent on the hydrogen content, and the hardness values increase with the hydrogen content increases. These results reflect that the hydride identified as the δ phase in the present study has a brittle property in the presence of stress, acting as a main source to increase the hardness value. This makes it possible to explain the detrimental effect of hydride on ductility of this alloy shown in Fig. 7, because the hardness would be intimately correlated with the ductility. With respect to the effect of heat treatment only on the hardness of this alloy, a reduction of the hardness value is observed. It is well known that the hardness is usually associated with the grain size, precipitates, impurity and so on. The heat treatment (500 °C/30min + 400 °C/120min) of this alloy in the temperatures of the α Ti-alloy region would induce the enlargement of grain and precipitates. These results indicate that the effect of the enlarged grain size on the hardness dominated the precipitation hardening as a result of the enlarged precipitation size. It is thus considered that the enlarged grain size by the heat treatment would be mainly responsible for the reduction of hardness value of the as-received PT-7M titanium alloy.

4. CONCLUSIONS

In the present study, the effect of hydride on the mechanical property of PT-7M titanium alloy has been determined. The following conclusions are drawn;

- 1) The hydride precipitation of δ phase (TiH_2) formed in PT-7M titanium alloy has a significant effect on ductility of this alloy, even if he shows little effect on the strength of this alloy.
- 2) The hydrides, especially in the radius direction of the alloy tube, offered a source for crack initiation and propagation during deformation, leading to the cleavage failure
- 3) The Hardness values of hydrogen charged alloys increased with increasing the hydrogen content, since the hardness would be intimately associated with the amount of hydride precipitates having a brittle property in the presence of stress.
- 4) There was little effect of the heat treatment (500 °C/30 min + 400 °C/120 min) on the tensile property of PT-7M titanium alloy, because this alloy would be finally heat-treated above 500°C in the α temperature range after the final pilgering stage in the manufacturing procedures.

ACKNOWLEDGEMENTS

This work has been supported by the Korean Ministry of Science and Technology.

REFERENCES

1. O.A. Kozhevnikov, E.V. Nesterova, V.V. Rybin and I.I. Yarmolovich: *J. Nuclear Mater.* 271&272 (1999) 472-477
2. Gorynin, I.V.: *Materials Science and Engineering*, A263 (1999) 112-116
3. M.L. Wasz, F.R. Brotzen, R.B. McLellan, and A.J. Griffin, Jr: *International Materials Reviews* 41 (1) (1996) pp. 1-12
4. J.C. Williams: *M Materials Science and Engineering*, A263 (1999) 107-111
5. D.G. Kolman and J.R. Scully: *J. Electrochem. Soc.* 143 (1996) 1847-1860
6. E. Rolinski, G. Sharp, D.F. Cowgill and D.J. Peterman: *J. Nuclear Mat.* 252 (1998) 200-208
7. G. Lutjering: *Materials Science and Engineering A263* (1999) 117-126
8. S.V. Gnedenkov, P.S. Gordienko, S.L. Sinebrukhov, O.A. Khrisanphova, and T.M. Skorobogatova: *Corrosion*, 56 (2000) 24-31
9. K. Nakasa and H. Satoh, *Corrosion Sci.*, 38 (1996) 457.
10. H.D. Kessler, R.G. Sherman and J.F. Sullivan: *J. Met.*, 7 (1955) 242-246
11. G.A. Lenning, J.W. Sprietnak, and R.I. Jaffee: *Trans. AIME*, 206 (1956) 1235-1240
12. D.A. Meyn, *Metall. Trans.*, 5 (1974) 2405.
13. J.C.M. Li, R.A. Oriani and L.S. Darken, *Z. Phy. Chem.*, 49 (1966) 271.
14. W.J. Pardee and N.E. Paton, *Metall. Trans.*, 11A (1980) 1301.
15. A.W. Sommer and D. Eylon, *Metall. Trans.*, 14A (1983) 2178.
16. A. San-Martin and F.D. Manchester, *Bull. Alloy Phase Dia.*, 8 (1987) 30-42

Table 1. Chemical composition of PT-7M titanium alloy (wt.%)

Ti	Al	Zr	V	Fe	Co	S	C	O	N	H
95.17	2.19	2.35	0.05	0.06	0.15	0.001	0.092	0.0769	0.0056	0.0047

Table 2. Hydrogen contents of as-received and hydrogen charged PT-7M titanium alloys

PT-7M	As-received	Charging time (min)					
		5	10	13	20	30	60
H content (ppm)	47	69	102	300	538	1174	2291

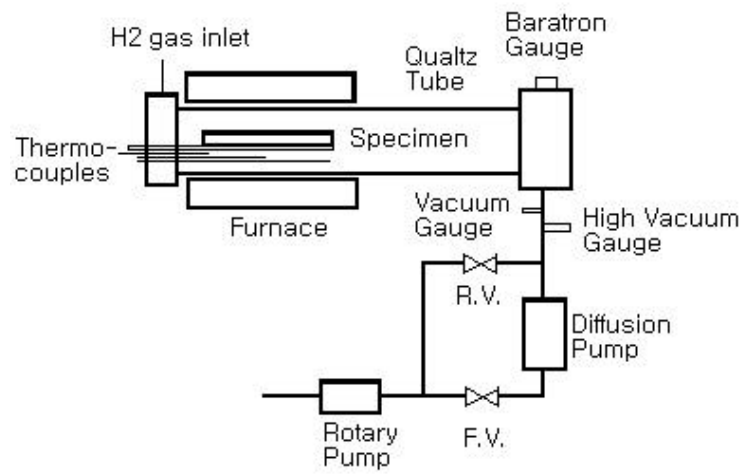


Fig. 1. Schematic diagram of hydrogen charging system.

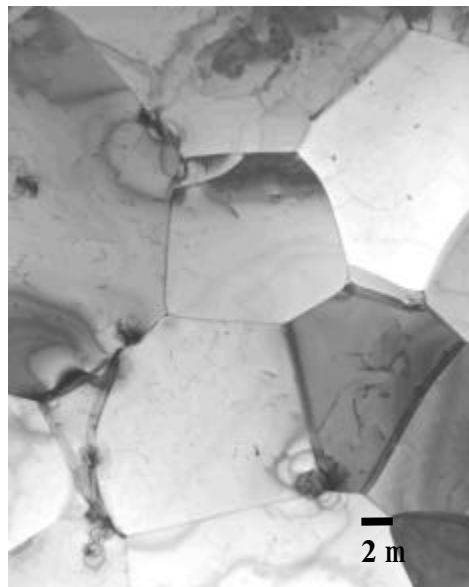


Fig. 2. Bright field TEM image of PT-7M titanium alloy.

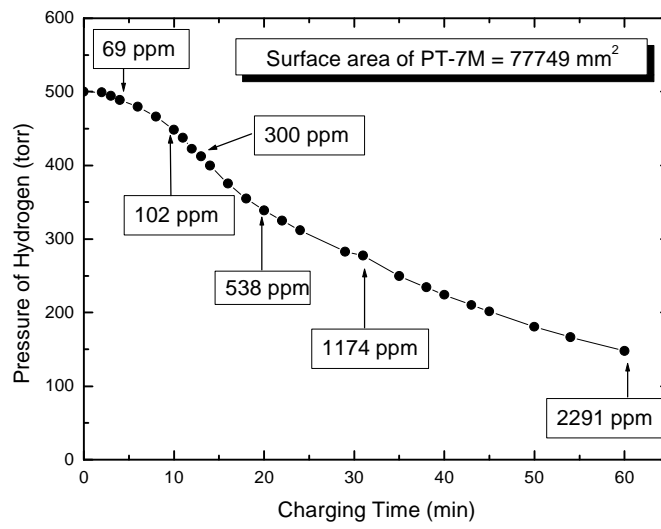


Fig. 3. Variation of hydrogen pressure with charging time.



(a)

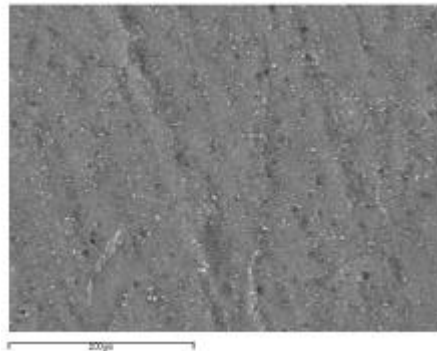


(b)

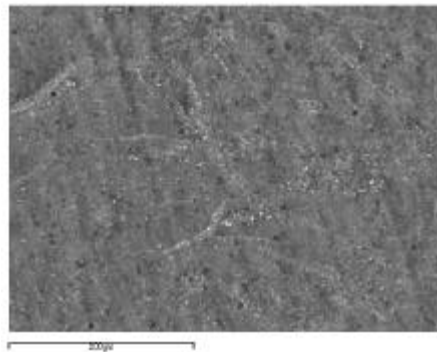


(c)

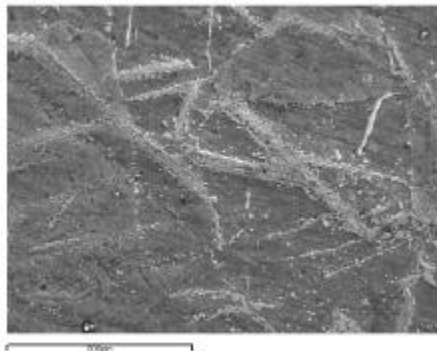
Fig. 4. Surface appearance of as-received and hydrogen charged PT-7M titanium alloy tubes: (a) as-received, (b) 1174 and (c) 2291 ppm.



(a)



(b)



(c)

Fig. 5. Microstructures of hydrogen charged PT-7M titanium alloys, showing hydride morphologies with hydrogen contents of (a) 102, (b) 538 and (c) 1174 ppm.

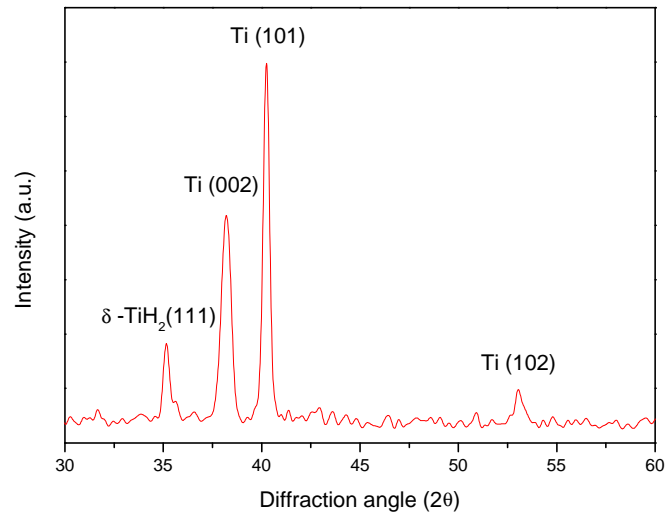


Fig. 6. X-ray diffraction pattern of hydrogen charged PT-7M titanium alloy with a hydrogen content of 1174 ppm.

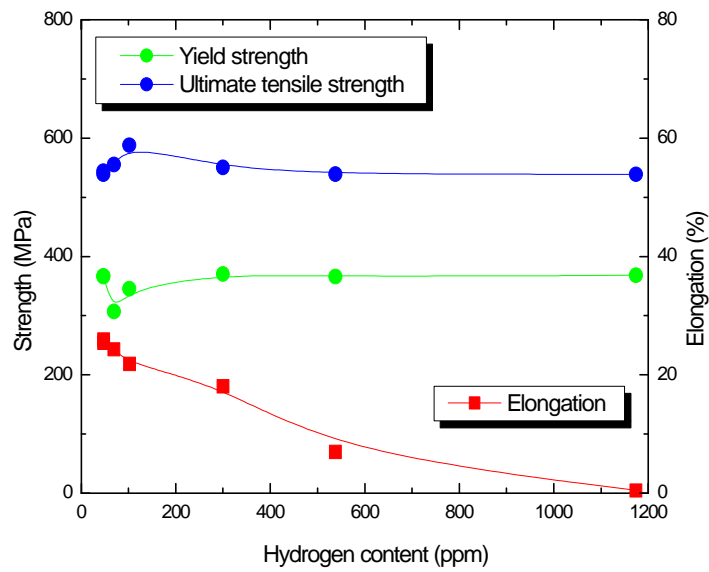
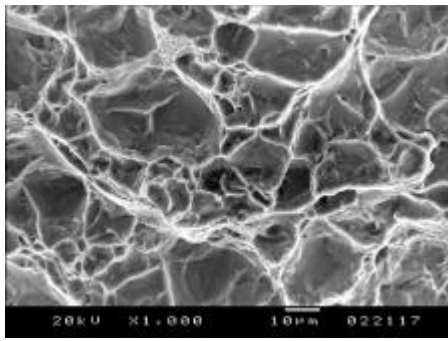
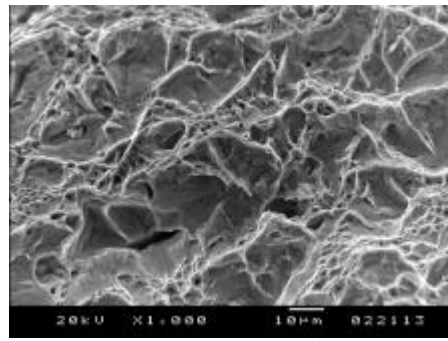


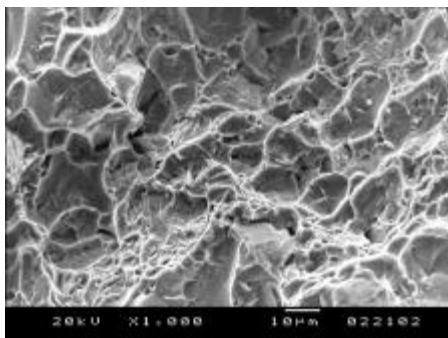
Fig. 7. Effect of hydrogen content on the mechanical property of PT-7M titanium alloy.



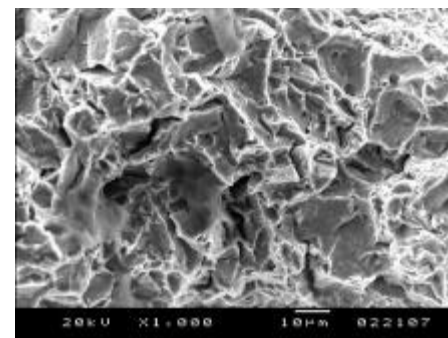
(a)



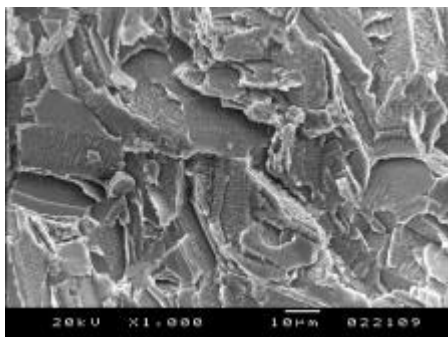
(b)



(c)



(d)



(e)

Fig. 8. Fractured surfaces of tensile tested PT-7M titanium alloys with hydrogen contents of (a) 47, (b) 69, (c) 102, (d) 300 and (e) 1174 ppm.

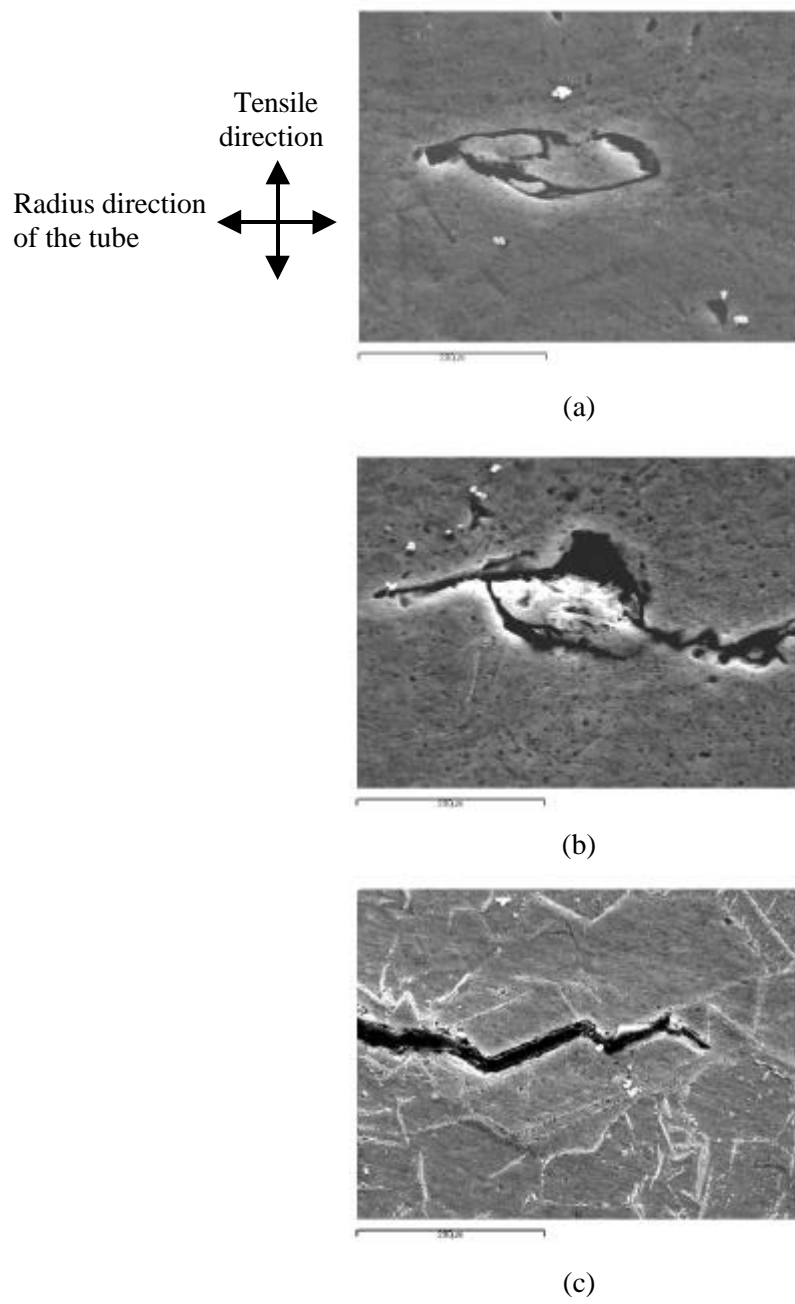


Fig. 9. Microstructures in the vicinity of the longitudinal sections of tensile tested PT-7M alloys with hydrogen contents of (a) 69, (b) 102 and (c) 1174 ppm.

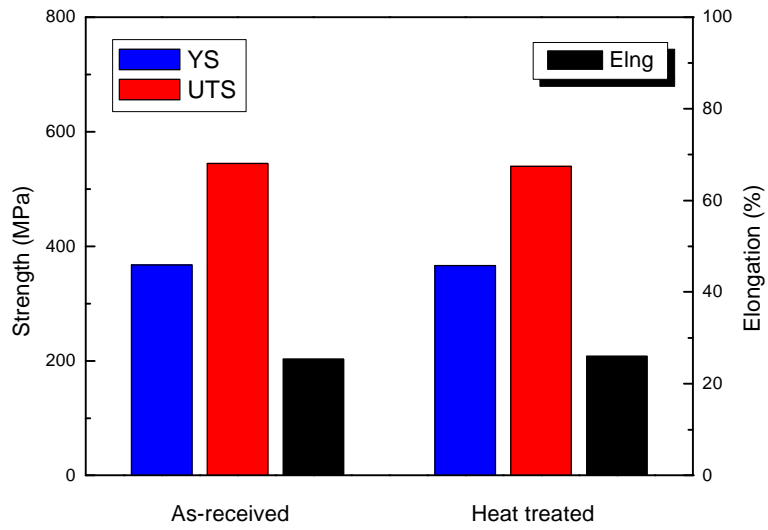


Fig. 10. Effect of heat treatment on the tensile property of PT-7M titanium alloy.

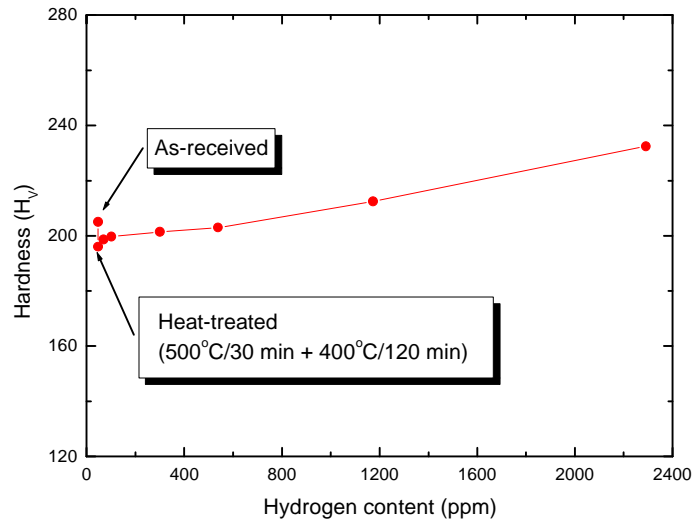


Fig. 11. Effect of hydrogen content on Vickers Hardness of PT-7M titanium alloy.